

1 Aging, rejuvenation, and thixotropy in yielding 2 magnetorheological fluids 3

4 Juan de Vicente · Claudio L. A. Berli

5 Received: 17 September 2012 / Revised: 27 March 2013 / Accepted: 4 April 2013
6 © Springer-Verlag Berlin Heidelberg 2013

7 **Abstract** The yielding behavior of dilute magnetorheological (MR) fluids has been investigated using creep–recovery tests. At very low stress levels, MR fluids behave in the linear viscoelastic regime as demonstrated by the fact that the instantaneous strain equals the instantaneous (elastic) recovery. In this region, gap-spanning field-induced structures support the stress levels applied. Upon increasing the stress value, the MR fluid evolves towards a nonlinear viscoelastic response. Here, the retarded elastic and viscous strain decrease, and the plastic contribution to the instantaneous strain grows probably due to the appearance of unattached field-induced structures. A larger stress value results in a viscoplastic solid behavior with negligible retarded and viscous strain and a fully plastic instantaneous strain. Finally, a plastic fluid behavior is found when the stress value is larger than the so-called yield stress. MR fluids exhibit an intermediate behavior between *non-thixotropic* (simple) and highly thixotropic model yield stress fluids.

25 **Keywords** Magnetorheology · Magnetorheological fluids · Creep · Recovery · Unsteady flow · Yielding · Phase diagram

Introduction

Magnetized magnetorheological (MR) fluids are known to exhibit nonequilibrium transitions from a fluid- to solid-like state, characterized by the sudden arrest of their dynamics. This phenomenology is ubiquitous to a wide variety of systems as already reported by Trappe et al. (2001). In this context, what makes MR fluids of especial interest is the fact that the jamming state of the constituent particles can be externally tuned by the application of magnetic fields. In other words, MR fluids can be considered smart attractive colloids as their interparticle (magnetic) attraction can be tuned externally.

In general, a colloidal system can be jammed by increasing the volume fraction of the constituents, increasing the interparticle attractions, or decreasing the stress. In this work, we will focus our attention in MR fluids that are jammed by increasing the magnetostatic interactions between the constituent particles for a constant volume fraction. Also, generally speaking, jammed solids have been reported to be refluidized by thermalization or by an applied stress, and consequently, a unified description has been proposed in terms of a jamming phase diagram for attractive colloidal particles that aimed to give a unifying link between the glass transition, gelation, and aggregation (Trappe et al. 2001). In this work, we are interested in unjamming the MR fluids under the application of shear stresses. Accordingly, we will be able to induce a solid- to fluidlike transition in MR fluids that are initially jammed at a given magnetic field strength and particle volume fraction, by simply applying a shear stress.

In rheological terms, jammed solids are typically identified by the appearance of a low-frequency plateau in the elastic modulus, a viscosity divergence, and eventually the

J. de Vicente (✉)
Department of Applied Physics, Faculty of Sciences,
University of Granada, 18071 Granada, Spain
e-mail: jvicente@ugr.es

C. L. A. Berli
INTEC (UNL-CONICET),
Güemes 3450, 3000 Santa Fe, Argentina

61 onset of a yield stress (the minimum stress value for the
62 material to flow) under the conditions of experimentation.
63 In spite of this apparently simple definition, the determi-
64 nation and also the existence of a true yield stress is still
65 controversial (Moller et al. 2006).

66 Probably the most suitable technique to measure a yield
67 stress is the so-called vane method (Barnes and Nguyen
68 2001). Unfortunately, the necessity of application of a
69 magnetic field precludes the use of this technique. How-
70 ever, in spite of its difficulty, there are many different
71 approaches to interrogate the yield stress in a MR fluid
72 that are also employed in other pasty materials (see for
73 instance Christopoulou et al. 2009; Laurati et al. 2011). In
74 most cases, the yielding behavior has been ascertained by
75 the application of shear stress or strain rate ramps. How-
76 ever, more reliable techniques have been employed in the
77 literature, for example, using stress/strain amplitude sweeps
78 (de Vicente et al. 2002, 2011). Among them, we would like
79 to emphasize the use of creep tests. In a creep test, a con-
80 stant shear stress is applied for a time interval, while the
81 strain is recorded. These are very delicate methods, espe-
82 cially when accompanied by a recovery stage and, at large
83 stresses, where tool inertia might prohibit instantaneous
84 halt. Consequently, the literature on this is very scarce.
85 Pioneering works that described the use of creep tests to
86 investigate the yielding behavior of MR fluids are briefly
87 summarized now. In 1994, Otsubo and Edamura (1994)
88 reported creep data on electrorheological (ER) fluids. They
89 showed that contrary to the expectation at that time, electri-
90 fied ER fluids did not behave as pure elastic solids at low
91 stresses but, instead, exhibited a retarded elastic and vis-
92 cous flow. Interestingly, the recovery behavior was found to
93 be purely plastic, for intermediate and large stresses, in dis-
94 agreement with classical single-chain model predictions. In
95 the ER fluids investigated, the yield stress value determined
96 by creep tests was found to be smaller than the plateau
97 stress in the flow curves. Li and coworkers (2002) investi-
98 gated the effect of magnetic field strength and temperature
99 on the creep behavior of MR fluids (below the yield value).
100 Their results indicated that MR fluids behaved as linear
101 viscoelastic bodies at very small stresses, with increas-
102 ing constant stresses, nonlinear viscoelastic, viscoplastic,
103 or purely plastic properties dominated. See et al. (2004)
104 also reported creep tests on commercial MR fluids in the
105 preyield regime. They demonstrated that shear compliance
106 data collapsed at low stresses, well within the linear vis-
107 coelastic region. The elastic compliance was best fitted by
108 a power law relationship $\propto H^{-4.4}$ in discrepancy with the
109 simple dipole–dipole interaction model that predicts a scal-
110 ing with H^{-2} . This finding was argued to reflect the fact
111 that as the magnetic flux density is increased, the nature of
112 structures themselves undergoes a change. In 2006, Chot-
113 pattanant et al. (2006) investigated the creep response of

poly(3-thiopheneacetic acid) ER fluids. They demonstrated 114
that similarly to MR fluids, the suspensions exhibited an 115
evolution with an increase of applied stress from a linear vis- 116
coelastic response at low stresses to a nonlinear viscoelastic 117
response, followed by a viscoplastic solid, and finally a 118
transition from plastic solid to plastic liquid at the yield 119
stress. 120

Creep–recovery tests have also been employed in the 121
examination of the yielding behavior of other pasty 122
materials. For example, creep–recovery measurements by 123
Petekidis et al. (2003, 2004) demonstrated that hard-sphere 124
(repulsive) colloidal glasses tolerate large strains, up to at 125
least 15 %, before yielding irreversibly. A non-negligible 126
recovery is found even in samples which have flowed sig- 127
nificantly during stressing. Such a recovery is attributed to 128
cage elasticity. The creep–recovery behavior of attractive 129
colloidal glasses was investigated by Pham et al. (2008). In 130
contrast to what occurred for hard-sphere colloidal glasses, 131
the recovered strain exhibits a peak with stress, and a finite 132
recovered strain is measured even well above the yield 133
stress. More recently, a similar peak was also found when 134
plotting the maximum recovered strain versus stress values 135
in the case of colloidal gels by Laurati et al. (2011). 136

In this work, we are interested in a better understanding 137
of the yielding behavior of MR fluids under the pres- 138
ence of uniaxial DC external magnetic fields. To do so, 139
we carry out an extensive rheological study that involves 140
steady and unsteady (shear) flows. Also, for a comparative 141
purpose, model yield stress fluids are formulated ad hoc 142
having similar yield stress values but exhibiting a very dif- 143
ferent thixotropic behavior. On the one hand, polyacrylic 144
acid polymers are employed as model microgel dispersions 145
that are essentially *non-thixotropic*. On the other hand, we 146
use bentonite clay suspensions that are well-known to form 147
very thixotropic yield stress fluids. Finally, time-dependent 148
changes in viscosity are explained in terms of the thixotropic 149
structural model developed by Quemada (2008). 150

151 Theory

Time-dependent rheological phenomena appearing in gels, 152
pastes, and colloidal glasses can be rationalized in terms 153
of structural viscosity models (Quemada 1998, 2008; 154
Derec et al. 2001; Coussot et al. 2002; Derec et al. 2003; 155
Craciun et al. 2003; Moller et al. 2009b). This kind of mod- 156
eling grounds is on three basic concepts: (a) a structural 157
variable S characterizing the structure, (b) a rate equation 158
of S that accounts for the forces perturbing the microstruc- 159
ture (viscous forces from the gradient velocity field) and 160
those restoring the equilibrium state (Brownian motion and 161
interparticle forces), and (c) a given form of the viscosity– 162
structure relation, $\eta(S)$. 163

164 In the model proposed by Quemada (1998), the structural
 165 state of dispersion is regarded as a mixture of individ-
 166 ual particles and clusters of them (structural units) sus-
 167 pended in a fluid. The structural variable S is defined
 168 as the number fraction of particles contained in the
 169 structural units. The time dependence of S results from
 170 the balance between buildup and breakdown of struc-
 171 tural units, which is governed by the following relaxation
 172 kinetics:

$$dS/dt = \left(t_{Br}^{-1} + t_{in}^{-1} \right) (1 - S) - t_{hy}^{-1} S \quad (1)$$

173 where t_{Br} , t_{in} , and t_{hy} are the characteristic relaxation
 174 times associated to Brownian, pair interaction, and hydro-
 175 dynamic forces, respectively. According to the definition
 176 given above, S enters the effective volume fraction of the
 177 disperse phase, $\phi_{eff} = \phi (1 + CS)$, where ϕ is the true
 178 particle volume fraction, and C is a compactness factor. It
 179 is observed that $\phi_{eff} \geq \phi$, because the effective volume
 180 fraction includes the volume occupied by the particles plus
 181 the volume of solvent immobilized hydrodynamically in the
 182 structural units. Finally, the shear viscosity is obtained by
 183 introducing $\phi_{eff}(S)$ into the following equation:

$$\frac{\eta}{\eta_F} = \left(1 - \frac{\phi_{eff}}{\phi_m} \right)^{-2} \quad (2)$$

184 which generalizes a relationship between viscosity and
 185 volume fraction for concentrated colloidal dispersions
 186 (Quemada 1977; Brady 1993; Heyes and Sigurgeirsson
 187 2004). In Eq. 2, η_F is the suspending fluid viscosity, and ϕ_m
 188 is the maximum packing fraction.

189 More recently, this modeling was extended to discuss
 190 time-dependent phenomena like thixotropy, aging, and reju-
 191 venation by inserting a time-dependent solution of the
 192 kinetic equation $S(t)$ in the viscosity relation $\eta(S)$ under an
 193 unsteady shear (Quemada 2008). The details of the result-
 194 ing “nonlinear structural” (NLS) model are not simple to be
 195 summarized, and the reader is referred to the original paper
 196 for further information. Here, we briefly describe the main
 197 rheological features that are of interest in the present work.

198 In the theoretical context of hard-sphere suspensions, if
 199 ϕ_{eff} is relatively high, the motion of structural units becomes
 200 strongly constrained due to the presence of neighbors, and
 201 the systems undergo a glassy transition when ϕ_{eff} reaches
 202 $\phi_g = 0.58$. If ϕ_{eff} further increases, the vibrational motion
 203 of particles vanishes at $\phi_m \approx \phi_{RCP} = 0.637$, the concen-
 204 tration of random close packing. Taking into account that
 205 ϕ_{eff} evolves in time, the model considers that the material
 206 is in a *fluid* phase for $\phi_{eff} < \phi_g$, and in a *paste* phase
 207 for $\phi_g \leq \phi_{eff} \leq \phi_{RCP}$. Furthermore, there exists a criti-
 208 cal volume fraction ϕ_{c2} that divides the paste domain into
 209 two: if the true volume fraction is $\phi < \phi_{c2}$, $\phi_{eff}(t \rightarrow \infty)$

remains lower than ϕ_m , the steady state viscosity is finite,
 and the system is called a *soft* paste. In contrast, if $\phi \geq \phi_{c2}$,
 $\phi_{eff}(t \rightarrow \infty)$ reaches ϕ_m , the viscosity *diverges*, and
 the material is called a *hard* paste. Therefore, for the system
 at rest, the NLS model predicts a *bifurcation* of the rheological
 behavior.

Accordingly, when the system is subjected to a constant
 shear stress τ , imposed after a destructuring step (preshear),
 the viscosity evolves as shown in Fig. 1a. For $\tau \leq \tau_Y$,
 the buildup of structure overcomes shear destructuring,
 and the viscosity tends to infinity. For $\tau > \tau_Y$, the structur-
 ing–destructuring processes attain a dynamical equilibrium,
 and steady viscosity plateaux are expected. As a consequence,
 a bifurcation is observed when τ reaches a critical value τ_Y ,
 which only exists for $\phi_{c2} \leq \phi \leq \phi_m$. For particle concen-
 trations lower than ϕ_{c2} , there is no sufficient structure to
 produce a bifurcation, even at zero shear stress.

As indicated in Fig. 1a, the region of $\tau \leq \tau_Y$ is asso-
 ciated to the phenomenon of *aging*, which is characterized

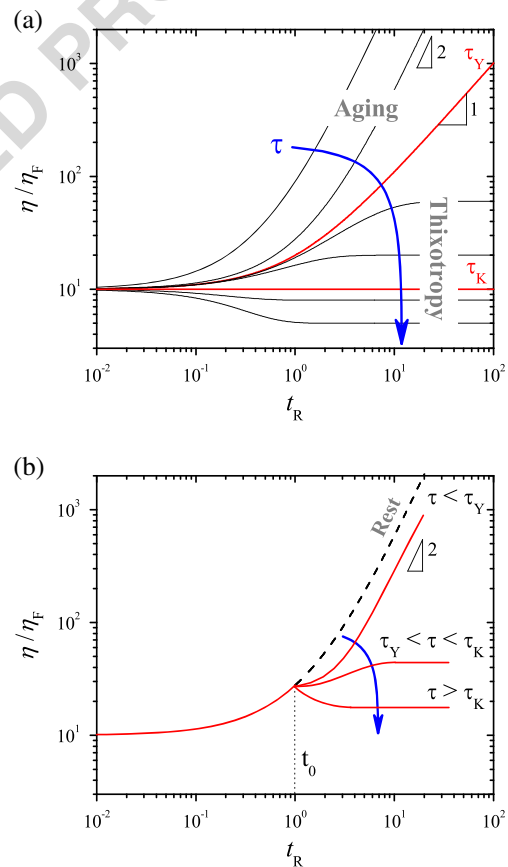


Fig. 1 **a** Relative viscosity as a function of dimensionless time, $t_R = t/(t_{Br} + t_{in})$, for *pastes* under constant shear stress, as predicted by Quemada’s model (Quemada 2008). Arbitrary values of model parameters were used in calculations to qualitatively illustrate the viscosity bifurcation phenomena. τ increases from *stop* to *bottom*. **b** Relative viscosity as a function of dimensionless time for *pastes* under constant shear stress after aging at rest

229 by the absence of equilibrium (no steady state viscosity is
 230 attained), and the slowing down of the evolution with a char-
 231 acteristic time that is proportional to the *age* of the system.
 232 Instead, the region of $\tau > \tau_Y$ corresponds the phenomenon
 233 classically known as *thixotropy*, where a steady state viscos-
 234 ity value is reached after a characteristic time that depends
 235 on Brownian motion and interparticle forces. Also in this
 236 region, the model predicts the existence of a stress τ_K where
 237 the system remains unaltered in its initial state ($S = S_{init}$).
 238 This stress value cannot be considered as an intrinsic charac-
 239 teristic of the material, since its value depends on the initial
 240 structure. When the stress $\tau_Y < \tau < \tau_K$, increasing the
 241 viscosity from its initial value corresponds to restructuring
 242 ($dS/dt > 0$). In contrast, when $\tau > \tau_K$, decreasing the
 243 viscosity from its initial value corresponds to destructuring
 244 ($dS/dt < 0$).

245 If the constant shear stress follows a rest period, depend-
 246 ing on its length, the initial structure changes. In general,
 247 the longer the rest time is, the larger is the structural
 248 variable S . Interestingly, in the NLS model, the stress bifurca-
 249 tion is intrinsically independent of initial conditions, in
 250 contrast to predictions of Coussot and coworkers (2002,
 251 2006). It is also possible that, depending on the material
 252 under study, the sample significantly ages during the rest
 253 period. Actually, this will be the case of highly thixotropic,
 254 bentonite clay suspensions studied in this work. If $\phi \geq$
 255 ϕ_{c2} , the material ages with a viscosity that grows as t^2 ,
 256 and there are three possibilities depending on the level of
 257 the stress applied (see Fig. 1b): (a) for very low stresses
 258 ($\tau < \tau_Y$), structuring continues with a viscosity that
 259 diverges as t^2 ; (b) for intermediate stresses ($\tau_Y < \tau < \tau_K$),
 260 structuring increases but reaches a finite value; and finally,
 261 (c) for very large stresses ($\tau > \tau_K$), a maximum is initially
 262 reached, and then the viscosity decreases to reach a steady
 263 value.

Q1 264 The steady state $\phi_{eff}(t \rightarrow \infty)$ response of systems with
 265 $\phi_{c2} \leq \phi \leq \phi_m$ subjected to $\tau > \tau_Y$ is that of fluids with a
 266 yield stress τ_Y . In this case, the model predicts the following
 267 steady shear viscosity:

$$\eta(\tau) = \eta_\infty \left(\frac{\tau + \tau_C}{\tau - \tau_Y} \right)^2, \quad (3)$$

268 where η_∞ is the high shear viscosity, and τ_C is a critical
 269 shear stress. Of course, if $\tau \leq \tau_Y$, $\eta \rightarrow \infty$ and $\dot{\gamma} = 0$.
 270 This nonlinear plastic behavior represents quite well several
 271 experimental results (see, for example, Berli and Quemada
 272 2000).

273 Finally, we mention the structural model proposed by
 274 Coussot et al. (2002), which also involves a structural
 275 variable that evolves following a linear kinetics, and is
 276 empirically related to the shear viscosity η . Despite this
 277 model lacks of a detailed description of the micro- or
 278 mesostructure, it is able to capture some features of the

macroscopic response, notably the viscosity bifurcation, 279
 and thus also helps to rationalize experimental results 280
 (Moller et al. 2006, 2009a). 281

Materials and methods 282

283 Conventional MR fluids were formulated by dispersing car-
 284 bonyl iron microparticles (HQ grade, BASF) in silicone
 285 oils (20 ± 3 and 487 ± 2 mPa·s, Sigma-Aldrich) with-
 286 out additives. The particle volume fraction was fixed at 5
 287 vol%. Accordingly, the MR fluid is expected to operate
 288 in the strong link concentration regime where the stor-
 289 age modulus increases with increasing the concentration,
 290 while the yield strain decreases with increasing the partic-
 291 le content (Segovia-Gutiérrez et al. 2012). This prevents
 292 complications that appear for larger concentrations where
 293 a two-step yielding process has been recently described
 294 (Segovia-Gutiérrez et al. 2012). Model yield stress fluids
 295 employed in the second part of this manuscript were pre-
 296 pared from aqueous dispersion of polyacrylic acid polymers
 297 (Sigma-Aldrich) and bentonite clay (Sigma-Aldrich). On
 298 the one hand, microgel suspensions were prepared from the
 299 neutralization of polyacrylic acid solutions at a concentra-
 300 tion of 0.5 wt%. On the other hand, the clay volume fraction
 301 was fixed at 10 wt%.

302 Rheology experiments were conducted in a stress-
 303 controlled MCR 501 magnetorheometer (Anton Paar) to
 304 explore the yielding behavior of MR fluids in the pres-
 305 ence of magnetic fields ranging from 52 to 259 kA/m.
 306 A plate–plate geometry (diameter 20 mm) was used. The
 307 temperature of the sample was stabilized at 25 °C using
 308 a circulating fluid bath. According to the manufacturer,
 309 the technical specifications of the rheometer were as fol-
 310 lows: the minimum and maximum torques were 0.1 μ Nm
 311 and 230 mNm, respectively. On the other hand, the mini-
 312 mum and maximum speeds (in CSS mode) were 10^{-7} and
 313 3,000 min^{-1} , respectively. It is worth to stress here that all
 314 experimental data reported in this study, although noisy in
 315 some cases, are well inside the specifications of the rheome-
 316 ter. Finally, it is worth to remark that slip was not observed
 317 during the experiments, and therefore, the rheometer tools
 318 were not surface treated (Segovia-Gutiérrez et al. 2012).

319 First, steady shear flow tests were carried out as
 320 described in Segovia-Gutiérrez et al. (2012). Briefly, the
 321 experimental procedure is summarized as follows: (a) ini-
 322 tially, the sample was preconditioned at a constant shear rate
 323 200 s^{-1} for 30 s; (b) next, the suspension was left to equi-
 324 librate for 1 min in the presence of a magnetic field; and
 325 (c) finally, the shear stress was logarithmically increased
 326 from 0.1 Pa at a rate of ten points per decade. Experiments
 327 were repeated at least three times with fresh new samples.
 328 The yield stress in the MR fluids is typically determined

329 using two different approaches. The first one consists in
 330 the determination of the so-called static yield stress as the
 331 stress corresponding to the onset of flow in double loga-
 332 rithmic representations of stress versus shear rate. A second
 333 method to determine the yield stress is to fit the Bingham
 334 plastic equation to a rheogram (shear stress versus shear
 335 rate) in lin–lin representation. The latter procedure results
 336 in the so-called Bingham yield stress that depends on the
 337 range of shear rates considered. Even though there are other
 338 more appropriate methods to measure the yield stress, these
 339 two approaches are frequently used in the MR literature
 340 (Volkova et al. 1999; de Vicente et al. 2002). For the purpose
 341 of this study, we are interested in the static yield stress.

342 Step stress and recovery tests were also performed under
 343 shear. The experimental protocol used is summarized in
 344 Fig. 2 as follows: (a) a preshear was first applied to eliminate
 345 shear history effects during 30 s (shear rate 100 s^{-1}); (b) an
 346 equilibration step followed at rest in a quiescent state (stress
 347 equal to zero), again during 30 s; (c) the magnetic field was
 348 suddenly applied during 120 s to promote the field-induced
 349 structuration; and (d) finally, step stress and recovery tests
 350 followed still in the presence of the magnetic field. In a

typical essay, a constant shear stress τ_0 was applied for a
 351 time of 300 s, while the resulting strain was measured. The
 352 stress was then removed, and the recovered strain was mea-
 353 sured for another 300 s. In all cases investigated, the strain
 354 was reset to zero at the beginning of the creep test.
 355

Steady shear rheology of MR fluids

Figure 3a shows steady shear flow curves for 5 vol% MR
 357 suspension in 20 mPa·s silicone oil under different mag-
 358 netic fields. In the absence of magnetic fields, the sample
 359 behaves as a Newtonian fluid (results not shown). However,
 360 in the presence of magnetic fields, the stress increases over
 361 the entire range of shear rates. In this figure, it is clearly
 362 shown that the MR fluid exhibits a yield stress, as a result
 363 of strong magnetic interactions among particles. The full
 364 lines in Fig. 3a represent Eq. 3, which is the steady state
 365 prediction of the structural viscosity model for effective vol-
 366 ume fractions entering the paste phase, therefore leading
 367 to a plastic-like behavior. Yield stress values in Fig. 3a are
 368 clearly defined and hence model-independent. It is worth
 369

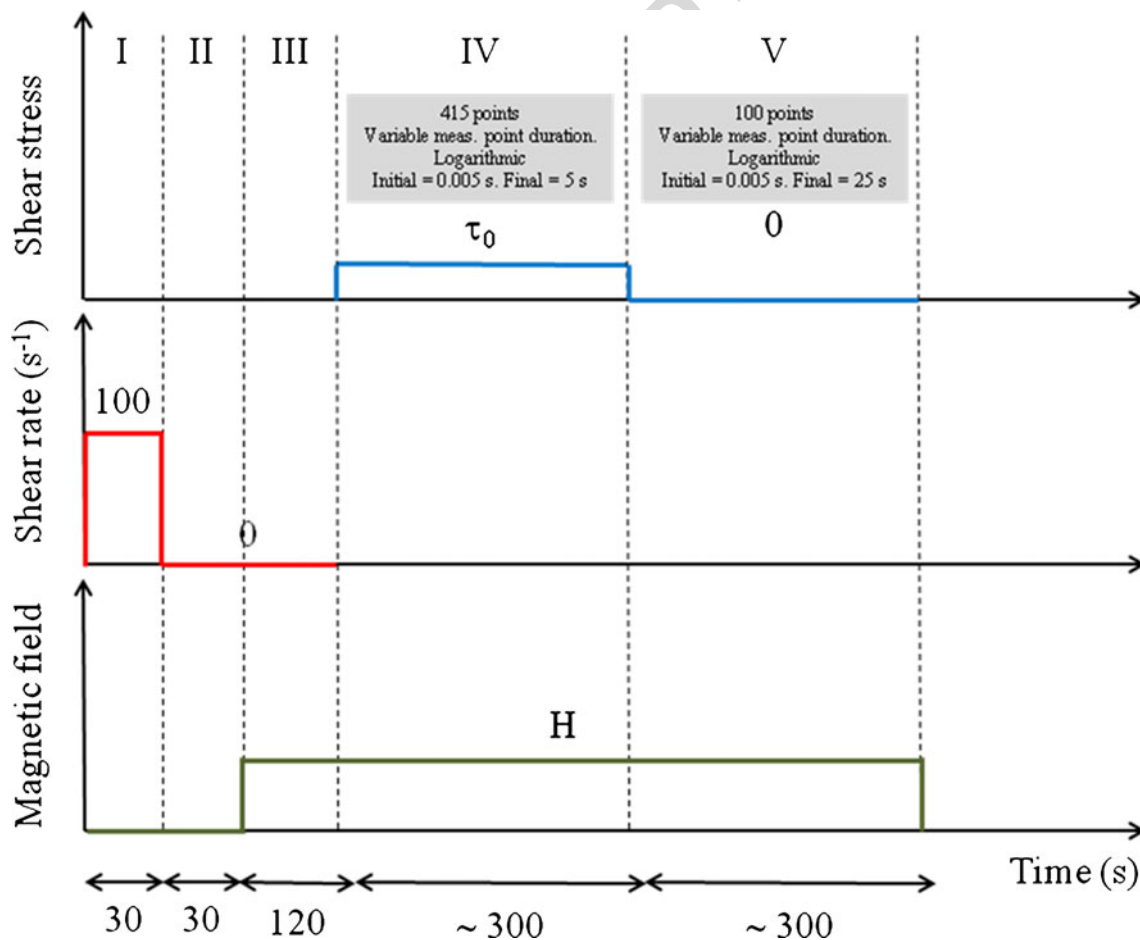


Fig. 2 Schematic of the protocol used for the creep–recovery investigations. Not to scale

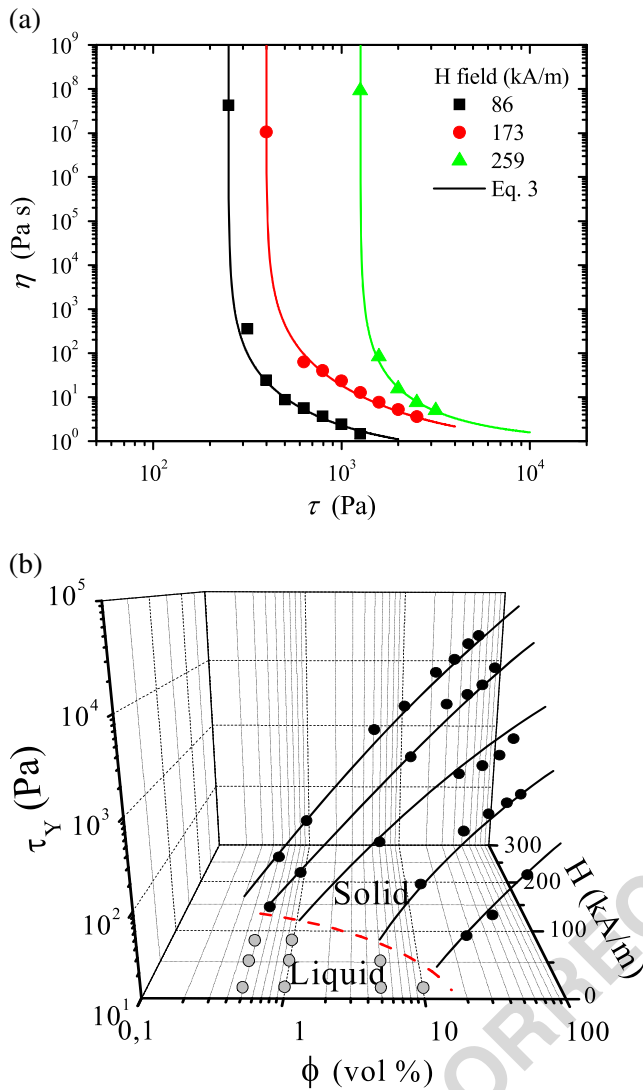


Fig. 3 **a** Steady shear flow curves for 5 vol% MR suspension in 20 mPa·s silicone oil in different magnetic fields. Symbols are experimental data. Full lines represent the structural viscosity model (Eq. 3; see text for details). **b** Three-dimensional jamming phase diagram for carbonyl iron-based MR fluids defined by the apparent yield stress (black symbols) as a function of both magnetic field strength and particle concentration (lines are used to guide the eyes). Gray symbols correspond to liquid states

370 noting, however, that the $\eta(\tau)$ trend of these suspensions
371 cannot be described by the linear Bingham model.

372 On the other hand, if the applied magnetic field is relatively
373 low (below ≈ 10 kA/m), the effective volume fraction
374 (particle aggregates) is not sufficiently high, and the system
375 is fluidlike for the whole range of shear rates and time
376 scales explored in the experiments (Segovia-Gutiérrez et al.
377 2013). Eventually, a low-shear Newtonian plateau could be
378 attained within an appropriate experimental window, as it
379 was discussed in a recent work (Berli and de Vicente 2012).

In collecting data from a series of experiments analogous to that reported in Fig. 3a, at different particle volume fractions, we were able to build a three-dimensional jamming phase diagram for carbonyl iron-based MR fluids, which is shown in Fig. 3b. This figure closely resembles that reported in Fig. 3, in Trappe et al. (2001), and suggests the applicability of the jamming transition in describing aggregated MR fluids for a fixed time scale. Projecting the data plotted in Fig. 3b (yield stress) over the ϕ -H-plane defines a phase boundary that visibly differentiates fluid- and solid-like states. The transition can be reached either by increasing ϕ at a constant attractive interaction energy or by increasing the strength of particle–particle interactions at a given value of ϕ . The second possibility is normally used in the practice with MR fluids, where the attractive interaction is controlled by means of the external magnetic field H. A similar phase diagram can be obtained from a series of magnetosweep tests at fixed particle concentrations (Segovia-Gutiérrez et al. 2012). The resulting phase diagrams are in qualitative good agreement with the one obtained from steady shear flow tests described above. However, now, the critical field is found to be less sensitive on the particle concentration and one order of magnitude smaller, probably due to the different time scales employed in both steady and dynamic oscillatory shear tests. These results are not shown here for brevity.

The phase diagram also illustrates that the higher the attractive interaction is, the lower is the critical concentration ϕ_c required to reach a solid-like state in agreement with Trappe et al. (2001). This remarkable feature can be accounted for as a diminution of ϕ_c with the strength of the interaction. In fact, high values of ϕ are required to reach the solid-like threshold when the magnetic attraction is weak, since flocs continuously reorganize to form relatively small, compact clusters that are not enough to crowd the system. At the other extreme, when the interaction is strong, particle aggregation yields large, loosely packed clusters that easily jam to form an elastic solid, even at low values of ϕ . The critical volume fraction ϕ_c defined by Trappe et al. (2001) corresponds to ϕ_{c2} in the structural model of Quemada (2008), i.e., the minimum concentration required to attain a divergence of the shear viscosity, for a given interaction energy.

One may conclude that Fig. 3b resumes the role of particle concentration, interaction energy, and shear stress in the solid-like transition of MR fluids. To our knowledge, the phase behavior of MR fluids had not been discussed in this scenario before. This is important from the fundamental point of view (one observes that MR fluids present a universal phenomenology sheared with colloidal suspensions, emulsions, and microgels) (Trappe et al. 2001; Christopoulou et al. 2009; Laurati et al. 2011) and also has consequences in practice (for example, it is evident that the

433 critical H depends on ϕ and vice versa, which is relevant to
 434 formulate MR fluids for a given purpose).

435 Yielding behavior of MR fluids from step stress tests

436 As a way of example, Fig. 4 shows typical creep curves
 437 at shear stresses of 50, 150, 250, 400, 600, 1,000, 1,500,
 438 and 1,800 Pa, measured at a magnetic field strength of
 439 173 kA/m. From Fig. 3a, the yield stress at 173 kA/m is esti-
 440 mated as c.a. 400 Pa under a steady flow. Hence, under the
 441 classical Bingham plastic point of view, for stresses below
 442 400 Pa, the MR fluid is expected to behave as a elastic
 443 solid. However, a close observation of Fig. 4 reveals three
 444 regions at the lowest stress values investigated: instan-
 445 taneous, retardation, and constant rate that are in contradic-
 446 tion with an elastic solid behavior. When the stress is first
 447 applied, there is a sudden, almost instantaneous increase of
 448 strain in less than 1 s. This is followed by a slight increase
 449 over the next 300 s. For the largest stresses investigated,
 450 a steady state regime is reached where the sample flows.
 451 The fact that the strain linearly increases with time at the
 452 longest times suggests the development of a viscous flow
 453 that will not be recovered upon cessation of the stress. It
 454 is of outstanding interest the observed stepwise increase
 455 in strain for a stress of 1,000 Pa (see inset in Fig. 4) that
 456 has been associated in the past to unstable flows and/or
 457 aggregation fragmentation processes. Similar observations
 458 have been reported for MR fluids by See et al. (2004)
 459 (see Fig. 3b in their paper) and in the case of ER flu-
 460 ids by Otsubo and Edamura (1994) (see Fig. 5 in their
 461 paper).

462 Typical recovery curves are also shown in Fig. 4. Inter-
 463 estingly, the deformation is very slightly recovered when
 464 removing the stress, in contrast to linear viscoelastic the-
 465 ory where the instantaneous elastic strain on the applica-
 466 tion and removal of stress must be the same. The instan-
 467 taneously recovered strain defined as the strain which the
 468 sample recovers instantaneously after the removal of the
 469 stress is very small. Also, the total recovered strain, defined
 470 as the difference between the strain at the end of the recov-
 471 ery period and the maximum strain attained at the end of
 472 the creep period, is essentially the same as the instan-
 473 taneously recovered strain. Since the strain is not completely
 474 recovered after the removal of the stress, the MR fluid is
 475 behaving as a purely plastic material, and the minimum
 476 (critical) stress associated to the onset of plasticity corre-
 477 sponds to the yield value. Since wall slip was not observed
 478 in the experiments, the plastic response is a consequence of
 479 bulk properties in the MR fluids. Interestingly, the instan-
 480 taneous initial deformation without elastic recovery cannot
 481 be explained by the single-width chain model. In contrast,
 482 the deformation and rearrangement of particles in thick
 483 columnar structures have been argued to be responsible for

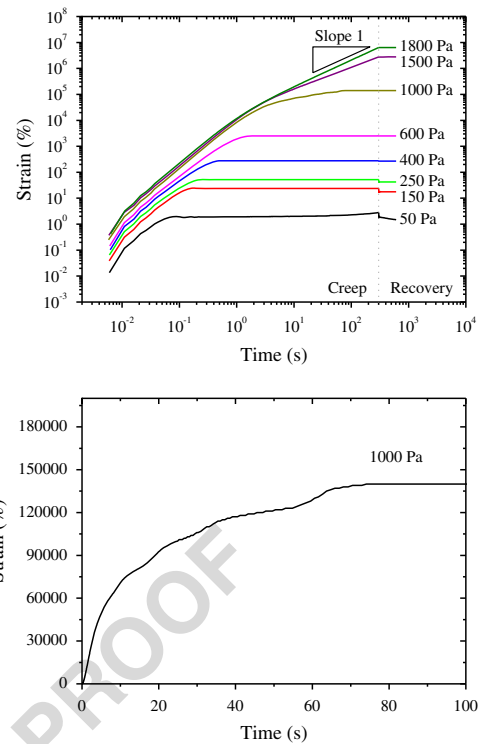


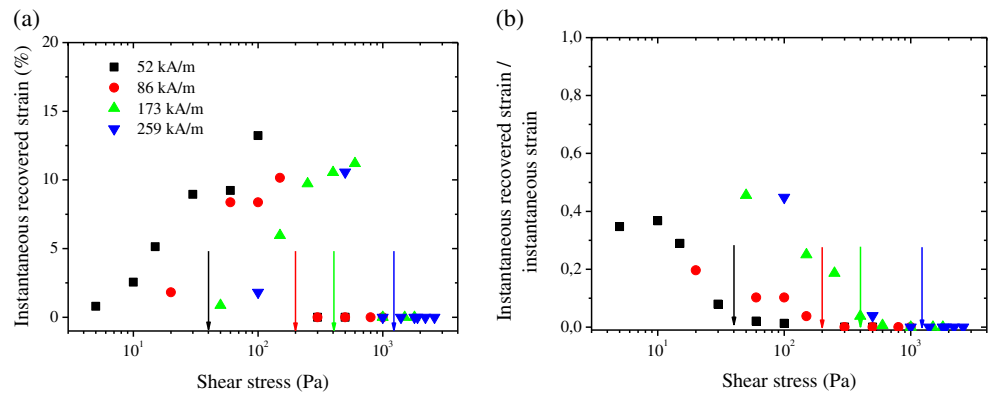
Fig. 4 Time dependence of the shear strain achieved during a step stress (creep) and recovery experiment at 5 vol% MR fluid for several stresses as indicated in the figure. The magnetic field strength is 173 kA/m

484 the purely plastic responses of MR fluids in the literature 484
 485 (Otsubo and Edamura 1994; Li et al. 2002; See et al. 2004). 485

486 More quantitative information on the yielding phenom- 486
 487 ena of MR fluids is obtained when plotting the instan- 487
 488 taneous, or the total recovered strain, as a function of 488
 489 the applied stress (Fig. 5) as it may give a measure of 489
 490 energy storage. As commented above, both magnitudes 490
 491 give extremely similar values. Results shown in Fig. 5a 491
 492 reveal that the recovered (elastic) strain is essentially pro- 492
 493 portional to the stress at low stress values. In fact, from this 493
 494 proportionality constant, at very low stress values, the stor- 494
 495 age modulus can be estimated (Petekidis et al. 2003). The 495
 496 instantaneous strain decreases with increasing the magnetic 496
 497 field strength. This was expected as the elastic modulus is 497
 498 known to increase with the magnetic field strength. Simi- 498
 499 lar results were obtained by Li et al. (2002) and See et al. 499
 500 (2004). 500

501 For large stresses, the total recovered strain reaches a 501
 502 maximum and then decreases. The maximum and, there- 502
 503 fore, the onset of nonlinearity are achieved at the same strain 503
 504 value (10 %) independently of the magnetic field employed. 504
 505 This finding is in good agreement with the crossover yield 505
 506 strain γ_C (i.e., the strain corresponding to $G' = G''$) reported 506
 507 by Segovia-Gutiérrez et al. (2012) and resembles the recov- 507
 508 ery observed for attractive colloidal glasses by Pham et al. 508

Fig. 5 Stress dependence of (a) the instantaneously recovered strain and (b) the ratio between the instantaneously recovered strain and the instantaneous strain. Vertical arrows correspond to the static yield stress as obtained from the extrapolation to zero shear rate of the flow curves in log–log representation (see Fig. 3b)



509 (2008) and colloidal gels by Laurati et al. (2011). This
 510 finding further implies that the energy required for particle
 511 arrangement is directly related to the strain level. The stress
 512 value corresponding to the transition from elastic deformation
 513 at small stresses to Newtonian flow at large stress (i.e.,
 514 at the maximum) is an indicator of the yield stress of the
 515 material. In fact, Fig. 5b demonstrates that there is a reason-
 516 ably good correlation between the stress values where
 517 the ratio between the instantaneously recovered strain and
 518 the instantaneous strain becomes zero and the yield stress
 519 obtained from steady shear flow curves (arrows in Fig. 5b).
 520 The recovery (elasticity) decreases with increasing the stress
 521 and reaches zero at the yield stress value. This finding is in
 522 good agreement with experiments on commercial MR fluids
 523 reported by Li et al. (2002). Also, with increasing the field
 524 strength at a fixed stress value, the viscoplastic response
 525 diminishes, and more elastic behavior ensues.

526 The creep and recovery behavior of MR fluids can be
 527 captured by using the generalized Kelvin–Voigt model that
 528 is constituted by a series association of a Maxwell liquid
 529 and a certain number of Kelvin–Voigt solids. According to
 530 this model, the creep compliance function can be written as
 531 (Tadros 1987) follows:

$$J(t) = \frac{\gamma}{\tau_0} = J_0 + \sum_{i=1}^N J_i \left(1 - e^{-t/t_i}\right) + \frac{t}{\eta_0} \quad (4)$$

532 and the recoil can be written as follows:

$$R(t) = \frac{\gamma_r}{\tau_0} = \frac{T}{\eta_{0r}} + \sum_{i=1}^N J_{ir} \left(e^{T/t_{ir}} - 1\right) e^{-t/t_{ir}} \quad (5)$$

533 Here, it is assumed that the stress is applied for $t < T$ and
 534 removed at $t = T$. Also, $t_i = \eta_i J_i$ represents the retard-
 535 ation time of the Kelvin–Voigt solid. For the experiments
 536 reported in this study, curves are well fitted, taking just one
 537 Kelvin–Voigt solid ($N = 1$). This description is particularly
 538 useful because all the data in the small strain region should

collapse to the shear compliance function if the MR fluid is
 539 responding in the linear viscoelastic regime. The first term
 540 in the RHS of Eq. 4 represents the elastic + plastic property
 541 of the MR fluid, the second term is associated to the delayed
 542 elastic strain, and finally, the third term is associated to the
 543 irreversible viscous flow. If the stress is applied for a long
 544 time, the sample may deform permanently, and the viscos-
 545 ity at the corresponding shear rate is given by the inverse
 546 of the slope of the compliance curves in this steady flow
 547 region. In the case of linear viscoelastic materials, J_0 must
 548 be elastically recovered upon cessation of the stress. How-
 549 ever, in magnetized MR fluids, J_0 generally comprises two
 550 components, an elastic one and a plastic one (see below).
 551

552 In Table 1, we show best-fitting parameters to Eqs. 4 and
 553 5 for a wide range of magnetic fields investigated. Data in
 554 Table 1 reveal that the instantaneous compliance slightly
 555 increases when the stress value for all magnetic fields inves-
 556 tigated increases. Strictly speaking, this point suggests that
 557 stresses applied are already out of the viscoelastic linear
 558 region. For all magnetic fields investigated, we could ideally
 559 identify three regions. (1) For low stresses, the compliance
 560 function has three contributions: instantaneous, retarded,
 561 and viscous flow. (2) Upon increasing the stress value, the
 562 retarded elastic and viscous components decrease, and at
 563 some critical stress, the MR fluid is instantaneously strained
 564 without the observation of retarded elastic and viscous com-
 565 ponents. At this stage, η_0 becomes infinite, and J_1 exhibits
 566 a very low negligible value (i.e., viscoplastic solid behav-
 567 ior). Similar findings were obtained by Otsubo and Edamura
 568 (1994). (3) For a larger stress value, $J_0 = 0$ and the MR
 569 fluid flows as a plastic fluid exhibiting a very low viscosity
 570 η_0 . The stress value corresponding to this transition has been
 571 associated in the past with the viscosity bifurcation phenom-
 572 ena observed by Coussot and coworkers (2002) in highly
 573 thixotropic yield stress materials, and as a consequence, this
 574 stress value may be considered the frontier between the pre-
 575 and postyield regimes. Even though non-negligible values
 576 are obtained from data fitting for J_1 and t_1 , the result of the
 577 fit is not sensitive to important changes in J_1 and t_1 .
 578

Table 1 Values of best-fitting parameters at each magnetic field strength according to Eqs. 4 and 5 t1.1

Stress (Pa)	Creep test				Recovery test			t1.2
	J_0 (1/Pa)	η_0 (Pa·s)	J_1 (1/Pa)	t_1 (s)	η_{0r} (Pa·s)	J_{1r} (1/Pa)	t_{1r} (s)	
52 kA/m								
5	0.0047	250,000	0.0012	16	64,000	0.001	14	t1.4
10	0.0065	410,000	0.00096	4.6	57,000	0.0021	0.46	t1.5
15	0.010	1,100,000	0.00156	2.6	32,000	0	–	t1.6
30 ^a	0.038	∞	0	–	8,400	0	–	t1.7
60 ^a	0.11	∞	0	–	2,700	0	–	t1.8
100	0	56	2.7	40	39	0	–	t1.9
300	0	5.2	20	78	3.8	0	–	t1.10
500	0	0.17	200	80	0.15	0	–	t1.11
86 kA/m								
20	0.0043	1,300,000	0.00039	1.8	78,000	0.00052	0.46	t1.12
60	0.012	∞	0.0016	1.9	25,000	0.00088	0.45	t1.13
100	0.0073	∞	0	–	42,000	0.00061	0.46	t1.14
150	0.018	∞	0	–	18,000	0.000092	0.45	t1.15
300 ^a	0	300	3.1	47	72	0	–	t1.16
500	0	18	4.7	50	14	0	–	t1.17
800	0	5.3	3.4	65	5.0	0	–	t1.18
1,000	0	3.4	3.0	68	3.3	0	–	t1.19
173 kA/m								
50	0.00038	1,900,000	0.000020	8.1	990,000	0.000089	87	t1.20
150	0.0015	∞	0.000074	0.9	250,000	0.000035	1	t1.21
250	0.0020	∞	0.00013	1.14	180,000	0.0001	0.5	t1.22
400	0.0062	∞	0.00077	1.85	45,000	0.0001	0.5	t1.23
600 ^a	0.042	∞	0.00057	11.28	7,200	0.00002	0.5	t1.24
1,000 ^a	0	∞	1.35	14.9	210	0	–	t1.25
1,500	0	18	2.05	41	16	0	–	t1.26
1,800	0	8.5	0	–	8	0	–	t1.27
259 kA/m								
100	0.00040	3,800,000	0.000011	1.3	1,100,000	0.000047	41	t1.28
500	0.0049	∞	0.00046	1.5	60,000	0	–	t1.29
1,000 ^a	0.097	∞	0.049	5.7	1,100	0	–	t1.30
1,400 ^a	0	∞	0.69	12	320	0	–	t1.31
1,800	0	60	1	30	51	0	–	t1.32
1,900	0	39	0.068	13	39	0	–	t1.33
2,200	0	16	0	–	15	0	–	t1.34
2,600	0	7.4	0	–	6.9	0	–	t1.35

Italicized values correspond to the fluidized (plastic fluid) region t1.36

^aMeasurements where a stepwise increase in strain is observed t1.37

578 Regarding the recovery behavior, we should say that the
 579 response is very slightly retarded as inferred from the low
 580 values of J_{1r} in Table 1. As a consequence, the recovery is
 581 nearly instantaneous and essentially given by the first term
 582 in Eq. 5 (T/η_{0r}). As observed in Table 1, η_{0r} decreases
 583 when the stress value independent of the magnetic field

strength increases. Importantly, a sudden drop in η_{0r} is
 584 observed at a shear stress close enough to the yielding point
 585 and associated to the maximum in Fig. 5a that manifests a
 586 purely viscous fluid flow. 587

It is also important to remark that stress values that are
 588 marked with an asterisk in Table 1 correspond to those 589

590 cases where a stepwise increase in the strain was monitored. Similar findings were reported in the past by Otsubo and Edamura (1994) and Li et al. (2002). This stepwise increase in the strain close to the critical yield stress value has been claimed to be due to field-induced chain rupture and reformation under shear.

596 Comparison between steady shear flow curves and creep tests: viscosity bifurcation
597

598 A further insight on the creep behavior can be obtained when plotting the instantaneous viscosity, defined as the ratio between the stress and the shear rate, as a function of time (see Fig. 6). This kind of representation has been traditionally employed (Coussot et al. 2002; Moller et al. 2006, 2009a) to investigate the yielding behavior of pastes and demonstrated the appearance of the previously commented viscosity bifurcation at the yield stress in the case of highly thixotropic yield stress fluids (Coussot et al. 2002) and a change in the viscosity versus time slope in the case of non-thixotropic yield stress fluids. Below the yield stress, the viscosity of non-thixotropic yield stress fluids keeps slowly increasing in time as $\eta \propto t^{0.6}$ for times even longer than 10^4 s (Moller et al. 2009b). In contrast, for non-thixotropic yield stress fluids above the yield stress, the viscosity quickly reaches a steady (constant) value. The structural models discussed above (Quemada 2008; Coussot et al. 2002) provide further insights to interpret these phenomena, at least qualitatively. Additional discussions are given below in relation to Fig. 12.

618 Results shown in Fig. 6 demonstrate a slow flow that appears to occur at long times in the preyield regime as indicated by the fact that the curves for the lowest stresses do not become perfectly horizontal lines but continue to rise ($\eta \propto t$). Even though these measurements are well inside the rheometer resolution, the very low values of the shear rate involved make this part of the measurement susceptible

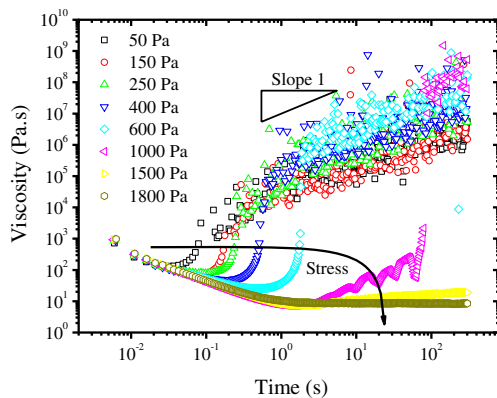


Fig. 6 Instantaneous viscosity as a function of time for constant stress values for 5 vol% MR fluid. The magnetic field strength is 173 kA/m

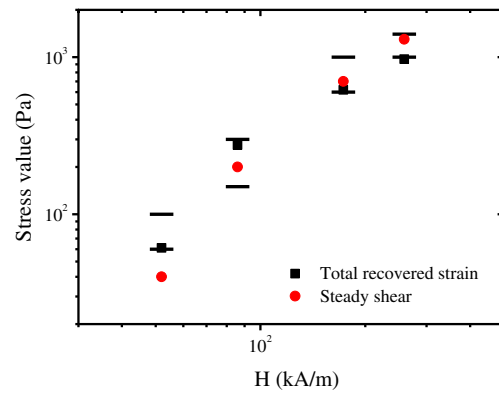


Fig. 7 Yield stress as a function of the external magnetic field in 5 vol% MR fluids. Horizontal lines correspond to the upper and lower bounds as obtained from viscosity bifurcation representations (Fig. 6). Squares correspond to those stresses where the ratio of recovered strains becomes zero (Fig. 5b). Circles represent the yield stresses obtained from the extrapolation in steady shear flow curves (Fig. 3b)

625 to possible sample slippage and instrument noise effects. Similar findings were reported for commercial MR fluids by See et al. (2004).

626
627
628 At this stage, it would be interesting to compare the yield stress obtained from steady shear flow curves and creep tests. In Fig. 7, we show such a comparison. As observed, steady shear and unsteady shear creep experiments provide yield stress data that are in reasonably good agreement. Actually, our results reveal that the yield value inferred from the maximum in the total recovered strain is in reasonably good agreement with the static yield stress obtained from steady shear flow curves. Contrary to our observations, Otsubo and Edamura (1994) reported a yield stress value from creep tests that were about 70 % of the plateau stress in steady shear flow curves.

640 Comparison with model yield stress fluids

641 As demonstrated above, MR fluids are yield stress fluids in the sense that they hardly flow if the imposed stress is below a certain (field-dependent) value, but they flow at high shear rates when the stress exceeds the so-called yield stress τ_Y .

642
643
644 It has been recently reported that yield stress fluids can be categorized in two groups: thixotropic and non-thixotropic (simple) yield stress fluids. Even though, in the past, the phenomena of yield stress and thixotropy have been considered separate fields of research, currently, they are demonstrated to be intimately linked (Moller et al. 2006; Coussot et al. 2006). On the one hand, an ideal simple (non-thixotropic) yield stress fluid is one for which the shear stress depends only on the shear rate. In this case, viscosity diverges continuously when the yield stress is approached from above. Typical examples involve foams, emulsions, and microgels. On the other hand, in (highly) thixotropic

657 yield stress fluids, the stress depends both on the (instan- 709
 658 taneous) shear rate and the shear history of the sample. By 710
 659 far, the vast majority of yield stress materials are highly 711
 660 thixotropic. In thixotropic materials, the stress reversibly 712
 661 decreases with time at high shear and increases with time 713
 662 under rest or low shear rates. As a consequence, a typi- 714
 663 cal test frequently used to ascertain whether a material is 715
 664 thixotropic or not is increasing the shear stress/rate and 716
 665 then decreasing it while continuously measuring the result- 717
 666 ing shear rate/stress. If the stress is not a function of the 718
 667 shear rate only but also depends on the history of the sam- 719
 668 ple, the two curves should not collapse, and the material is 720
 669 said to be (highly) thixotropic. Typical examples of (highly) 721
 670 thixotropic materials are clay suspensions and colloidal 722
 671 gels. 723

672 According to the discussion above, a carefully controlled 724
 673 measurement protocol must be followed to get reliable and 725
 674 reproducible results. As a consequence, prior to a test, yield 726
 675 stress fluids must be brought to the same initial state by a 727
 676 controlled history of shear and rest in what rheologists call 728
 677 a “preshear” stage. 729

678 Two model yield stress materials are employed in this 730
 679 work to compare their yielding behavior with that of con- 731
 680 ventional MR fluids. On the one hand, polyacrylic acid- 732
 681 based microgel suspensions are employed as a representa- 733
 682 tive example of simple yield stress fluids because they are 734
 683 very slightly thixotropic. On the other hand, bentonite clay 735
 684 suspensions are used as model (highly) thixotropic fluids. 736
 685 The particular formulations of these colloidal systems were 737
 686 chosen ad hoc for them to have a similar yield stress value 738
 687 under the same experimental conditions. 739

- 688 1. Microgel suspensions employed in this work are 740
 689 highly cross-linked anionic polyacrylic acid (PA) that 741
 690 swells upon neutralization to form electrically charged 742
 691 particles of approximately a few microns diameter 743
 692 (de Vicente et al. 2006; Gutowski et al. 2012). Con- 744
 693 centrations of approximately 0.1 wt% are reported in 745
 694 the literature to be sufficient for the particles to jam 746
 695 together to form a yield stress fluid. The weight concen- 747
 696 tration employed was 0.5 wt%. The pH was adjusted by 748
 697 adding sodium hydroxide. 749
- 698 2. Weakly flocculated clay suspensions were prepared by 750
 699 dispersion of bentonite clay (BC) in water. The weight 751
 700 concentration employed was 10 vol%. The reason for 752
 701 this concentration value is that the yielding behav- 753
 702 ior of these particular systems has been extensively 754
 703 reported in the literature. Actually, data for increas- 755
 704 ing and decreasing stress ramps have been reported by 756
 705 Moller et al. (2009a). 757
- 706 3. Unless appropriately stabilized, MR fluids are well- 758
 707 known to exhibit important sedimentation problems 759
 708 because of the large density mismatch between the con-

stituent iron particles and dispersing medium. To ensure 709
 that MR fluids remain stable at least during the rheology 710
 tests and, in particular, during the quiescent period at the 711
 preshear stage, we did increase the viscosity of the dis- 712
 persing medium. Hence, silicone oils employed in the 713
 formulation of MR fluids employed in this section had 714
 a viscosity of 487 mPa·s. By simply increasing the vis- 715
 cosity of the dispersing medium, iron microparticles are 716
 expected to remain in suspension in longer periods of 717
 time, and importantly, the yield stress is not expected to 718
 be much influenced at a given magnetic field strength. 719
 The particle concentration remained fixed at 5 vol%. 720
 When dealing with MR fluids, magnetic fields applied 721
 were 53 kA/m in order for the yield stress to be of a 722
 similar order of magnitude than the yield stress of PA 723
 and BC suspensions. 724

725 *Steady shear flow*

Getting reproducible results is notoriously difficult, espe- 726
 cially with highly thixotropic yield stress fluids, because 727
 of their shear history. Consequently, a strict experimen- 728
 tal protocol was followed to ensure reproducibility and 729
 comparability. Steady shear flow curves were ascertained 730
 following the protocol described in Fig. 8. For initial con- 731
 ditioning, the samples were subjected to steady shearing at 732
 100 s⁻¹ for 200 s and left (magnetized if needed) in a qui- 733
 escent state for 200 s. Subsequently, the test was started. To 734
 confirm that 200 s was sufficiently long for the microscopic 735
 structures to form, a series of tests were carried out using 736
 different intervals of time in the quiescent state. It is worth 737
 to stress here that a preconditioning is absolutely necessary 738
 to get reliable and reproducible results. Steady shear flow 739
 curves were obtained here using stress- and strain-controlled 740
 modes in order to more clearly differentiate between the 741
 so-called static and dynamic yield stresses. 742

Results obtained using the protocol described in the 743
 above paragraph are shown in Fig. 9 for the three systems 744
 investigated. In the case of PA, we clearly observe that both 745
 up and down stress curves do essentially overlap, suggesting 746
 that under the experimental conditions, microgel suspen- 747
 sions behave as non-thixotropic yield stress fluids. Note that 748
 in this case, the stress increases/decreases 1 Pa every 3 s, 749
 and this is a long time enough for the microgel suspension 750
 to reach a pseudo-steady state. As we will see later, the 751
 steady state is reached in only 1 or 2 s (see Fig. 10a). Impor- 752
 tantly, the non-thixotropic character is manifested by using 753
 both stress- and strain-controlled tests. Actually, the steady 754
 shear rheology of PA microgels is fit extremely well by 755
 the Herschel–Bulkley model (Moller et al. 2006; 2009a, b; 756
 Gutowski et al. 2012). As shown in Fig. 9a, the yield stress 757
 of PA suspensions is around 20 Pa. As expected, this is a 758
 much smaller value than the Bingham one predicted from 759

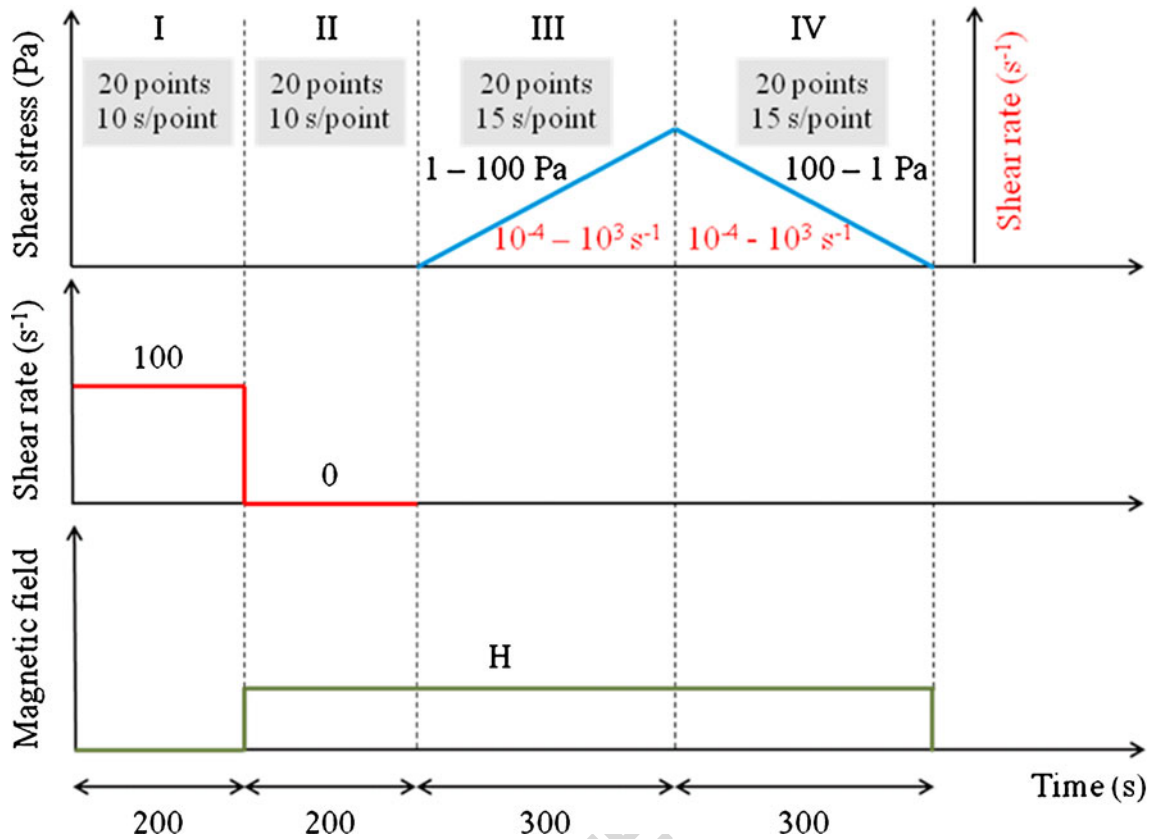


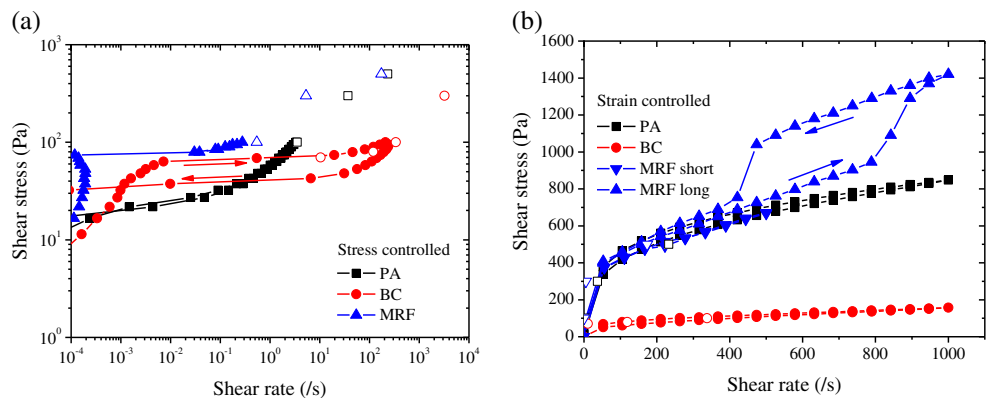
Fig. 8 Schematic of the protocol used for the steady shear flow curve investigations. Not to scale

760 lineal regression, at large deformation, to stress/shear rate
761 data in Fig. 9b.

762 Similar to PA suspensions, data for increasing and
763 decreasing shear stresses in MR fluids coincide (cf. Fig. 9a).
764 These results are further checked through strain-controlled
765 tests up to shear rates of 400 s^{-1} (cf. “MR fluid (MRF)
766 short” data in Fig. 9b). As a consequence, a priori MR flu-
767 ids formulated here in a high viscosity dispersing medium
768 can be considered as non-thixotropic yield stress materi-
769 als. In our case, the static yield stress in MR fluids is
770 around 70 Pa (cf. Fig. 9a), while the dynamic/Bingham

771 yield stress value is found to be very similar to that of
772 PA suspensions (approx. 500 Pa, cf. Fig. 9b). For com-
773 pleteness, in Fig. 9b, we include up-and-down shear rate
774 ramps covering a larger shear rate range (up to $1,000 \text{ s}^{-1}$)
775 where the isotropic–nematic transition for MR fluids is
776 observed (for further details, see Volkova et al. 1999). For
777 the purpose of the present study, we are only interested
778 in the early stages of the yielding process, and conse-
779 quently, we will not achieve large enough shear stresses
780 (shear rates) for the development of the isotropic–nematic
781 transition.

Fig. 9 Up-and-down stress curves of (a) stress controlled, (b) strain controlled. Open symbols correspond to steady shear viscosity values obtained from Fig. 10



782 Finally, BC suspensions do clearly exhibit a thixotropic
 783 loop. This was expected as the weakly flocculated clay
 784 suspension liquefies at high stresses, and then, the branch
 785 obtained upon decreasing the stress is significantly below
 786 the one obtained while increasing the stress. This is clearly
 787 seen in the kind of representation employed in Fig. 9a. Note
 788 that contrary to PA suspensions, in this case, 3 s is not
 789 enough for the BC suspensions to reach a steady state (see
 790 Fig. 12b in the following sections). The yield stress for BC
 791 suspensions as obtained from the up stress curve is very
 792 similar to that obtained for MR fluids (approx. 60 Pa).

793 It is worth to stress here that employing a lower viscosity
 794 silicone oil in the formulation of the MR fluid would result
 795 in a false thixotropic behavior due to the sedimentation of
 796 field-induced structures in the down curve. As demonstrated
 797 in Fig. 9a, the use of a larger viscosity dispersing medium
 798 prevents such sedimentation. It is also important to report
 799 that, a priori, the yielding behavior of MR fluids should
 800 not depend on the viscosity of the dispersing liquid as soon
 801 as the particle concentration and magnetic field strength
 802 remain constant. As will be shown later, the yield stress
 803 value for MR fluids formulated with different oil viscosities
 804 is essentially the same in spite of using different preshearing
 805 protocols.

806 *Creep–recovery tests*

807 Creep tests were also carried out in model yield stress flu-
 808 ids using the same preconditioning protocol (stages I and
 809 II in Fig. 8) as described above and with the same acqui-
 810 sition times as reported in Fig. 2. Additionally, we did also
 811 check that running concatenated creep/recovery tests after
 812 step V in Fig. 2 gave the same results for PA and MR flu-
 813 ids which were found to be non-thixotropic materials. On
 814 the other hand, as expected because of their thixotropic
 815 behavior, in the case of BC suspensions, concatenated
 816 tests gave different results because of the aging of the
 817 suspension.

818 Results obtained for PA-based (simple) yield stress flu-
 819 ids are shown in Fig. 10a. As observed, a few seconds after
 820 the shear stress is applied, the viscosity seems to reach a
 821 steady value for the larger stresses applied. However, for low
 822 stresses, curves obtained seem to deviate from this observa-
 823 tion. The observed transitional stress is interpreted in the
 824 literature as the yield stress. In the classical rheology litera-
 825 ture, this kind of simple yield stress fluid has been taken
 826 as an example to show that yield stress materials do not
 827 really exist but, instead, behave as very high viscosity ma-
 828 terials at low shear (Barnes 1999). However, more recently,
 829 this observation has been questioned (Moller et al. 2006) by
 830 running creep measurements for times as long as 10^4 s in
 831 nonslip samples. In the time interval investigated here, the
 832 viscosity value seems to reach a clear steady plateau value

for large stresses. On the other hand, similar to Moller et al. 833
 (2006), a slow flow appears here to occur at long times in the 834
 low stress regime that is well inside the rheometer’s resolu- 835
 tion. For these low stresses, the viscosity has been reported 836
 to increase with time following a power law with exponents 837
 that range from 0.6 for 2 % Carbopol suspensions to 1.0 for 838
 hair gels (Moller et al. 2009a). This increase with time is 839
 generally found to be independent of the stress value and is 840
 associated to *overaging* of the sample. 841

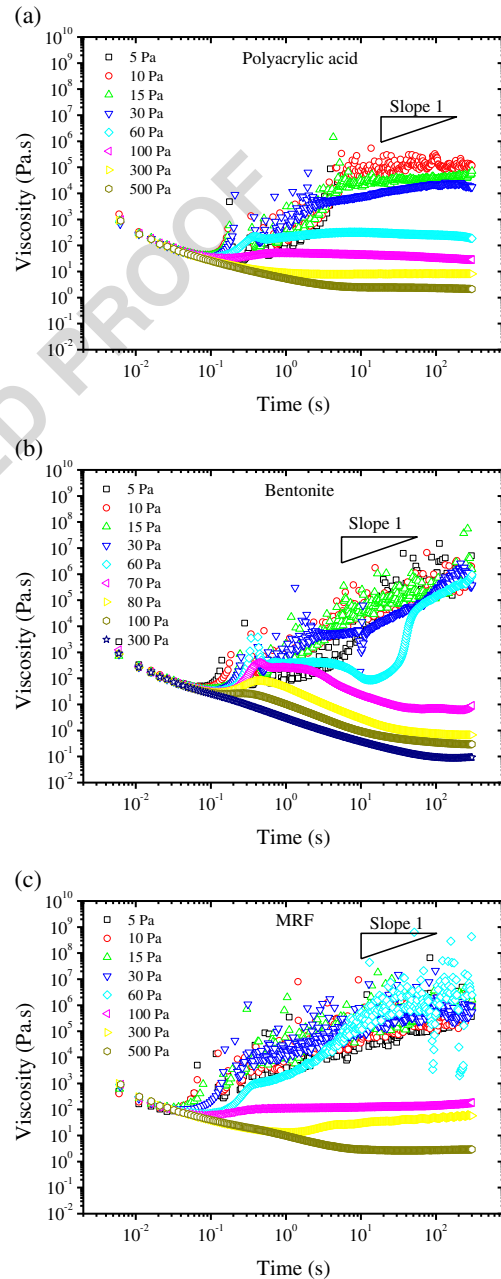


Fig. 10 Instantaneous viscosity as a function of time for different imposed stresses. **a** Microgel suspension, **b** clay suspension, **c** MR fluid

842 At this point, one should note that, strictly speaking,
 843 microgels are not free of thixotropy but present character-
 844 istic structuring times that are much shorter than those
 845 of bentonite clay suspensions, which is included here as
 846 a model thixotropic fluid (see Fig. 10b and discussions
 847 below). The subtle thixotropic behavior of microgels does
 848 not manifest in the timescales of the experiment associ-
 849 ated to Fig. 9 but becomes evident in Fig. 10a, where one
 850 observes that the system takes times around 1 s to reach the
 851 equilibrium viscosity, for the highest stresses applied.

852 Results for BC suspensions are included in Fig. 10b.
 853 This kind of representation highlights the viscosity bifur-
 854 cation and avalanche phenomena characteristic of (highly)
 855 thixotropic yield stress fluids such as BC suspensions.
 856 Contrary to what occurs in the case of microgel suspen-
 857 sions, now the viscosity very clearly increases with time
 858 at low stresses, and a non-monotonic behavior is observed
 859 for intermediate stress levels. It has been reported in the
 860 past that buildup (aging) of the structure wins over the
 861 destruction (rejuvenation) of it when thixotropic yield stress
 862 fluids are subjected to low stress values (below a critical
 863 yield stress). As a consequence, the shear rate enormously
 864 decreases, and hence, the viscosity increases quadratically
 865 in time “until the flow is halted altogether” (Moller et al.
 866 2006; Quemada 2008). On the other hand, for slightly larger
 867 stress values than the yield stress, the viscosity decreases by
 868 many orders of magnitude in an avalanche mode describ-
 869 ing a discontinuous transition (viscosity bifurcation). In
 870 terms of the structural model (Quemada 2008), the viscosity
 871 plateaux for $\tau > \tau_Y$ involve a dynamic equilibrium between
 872 structuring and destructuring processes, i.e., $dS/dt = 0$.
 873 The system may approach the equilibrium by either break-
 874 ing down ($dS/dt < 0$) or building up ($dS/dt > 0$) the
 875 structure. At intermediate shear stresses, the plateaux appear
 876 to be instable, which may be due to the high sensitivity to
 877 the imposed shear stress values in the close vicinity of the
 878 bifurcation (Fig. 1b). An outstanding difference when compar-
 879 ing Fig. 10a, b comes from the appearance of a shoulder
 880 in the case of BC suspensions. This can be easily explained
 881 because the suspension ages during the rest stage as demon-
 882 strated in Fig. 9a. Hence, for large enough stresses, $\tau > \tau_K$,
 883 viscosity must decrease to reach a steady value (see Fig. 1b).
 884 Experimental data corresponding to the MR fluids are

885 included in Fig. 10c. Results obtained qualitatively behave
 886 in an intermediate way between PA and BC suspensions
 887 and closely resemble measurements carried out in sec-
 888 tions above where the effect of magnetic field strength was
 889 explored. A quick look to the figures reveals that the low
 890 stress behavior of MR fluids is very similar to the one of
 891 BC suspensions. On the other hand, the high shear stress
 892 regime looks more alike to the PA suspensions. In other
 893 words, Fig. 10c shows that the viscosity of MRF quickly
 894 reaches a steady value for the larger stresses imposed, which

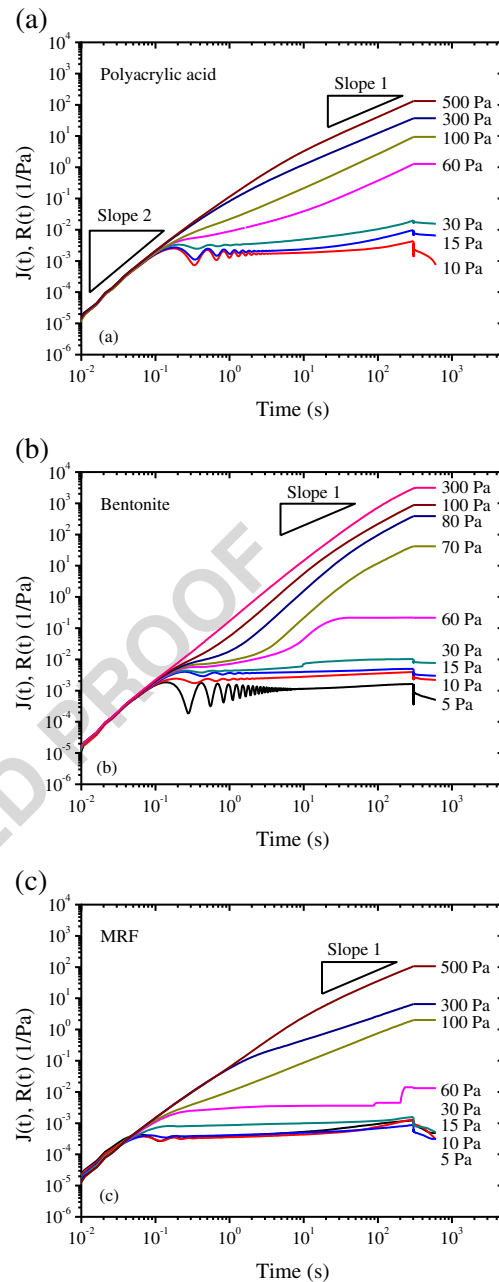


Fig. 11 Time dependence of the shear creep compliance $J(t)$ and recoil $R(t)$ functions for the three systems investigated: **a** microgel suspension, **b** bentonite suspension, **c** MR fluid. The initial noise in the compliance at low stresses is presumably caused by inertio-elastic effects

895 is a characteristic of systems virtually free of thixotropy, as
 896 discussed above for PA suspensions. However, at the low-
 897 est stresses, the viscosity continuously increases during the
 898 times observed, and the fluid seems to age similar to BC
 899 suspensions.

900 Again, more valuable information can be obtained in terms
 901 of the compliance and recoil functions corresponding to the
 902 creep and recovery stages. Results obtained for the three
 903

903 systems investigated are included in Fig. 11. This kind of
 904 representations clearly manifests the differences described
 905 above. The quadratic dependence of the strain with the time
 906 and the oscillations at short times may correspond to the
 907 response of the (viscoelastic) material when it is suddenly
 908 submitted to a shear stress, while there is a significant inertia
 909 of the system. In fact, a similar ringing has been described
 910 in the literature in the past in other different materials (e.g.,
 911 Coussot et al. 2006).

912 To get further information, compliance and recoil curves
 913 shown in Fig. 11 were fitted to Eqs. 4 and 5. The parameters
 914 obtained from the fits are included in Table 2. As observed
 915 in Table 2, the instantaneous compliance remains at a very
 916 low constant value for the lowest stresses investigated. This
 917 suggests that in this case, the systems essentially behave in
 918 the viscoelastic linear region. In Fig. 12a, we show that in
 919 spite of this, the behavior of the three systems under the

viscoelastic linear region (for a given stress value applied of 920
 15 Pa) is pretty different. On the one hand, the smallest η_0 is 921
 obtained for PA suspensions. On the other hand, the largest 922
 J_0 is obtained in the case of MR fluids. 923

924 The fact that the suspensions behave in the viscoelastic
 linear region is further confirmed in Fig. 12b where we find 925
 a quantitative good agreement between the low strain stor- 926
 age modulus (solid line in Fig. 12b) and the instantaneous 927
 strain/applied stress relation from creep tests (symbols in 928
 Fig. 12b) up to stress values of approximately 30 Pa. Again, 929
 this finding is also in good agreement with the fact that 930
 the instantaneous strain coincides with the instantaneously 931
 recovered strain at low stress levels (see Fig. 12c). Finally, 932
 deviation from linearity is also achieved at a very similar 933
 stress (≈ 60 Pa) and strain ($\approx 10\%$) levels (cf. Fig. 12d). 934

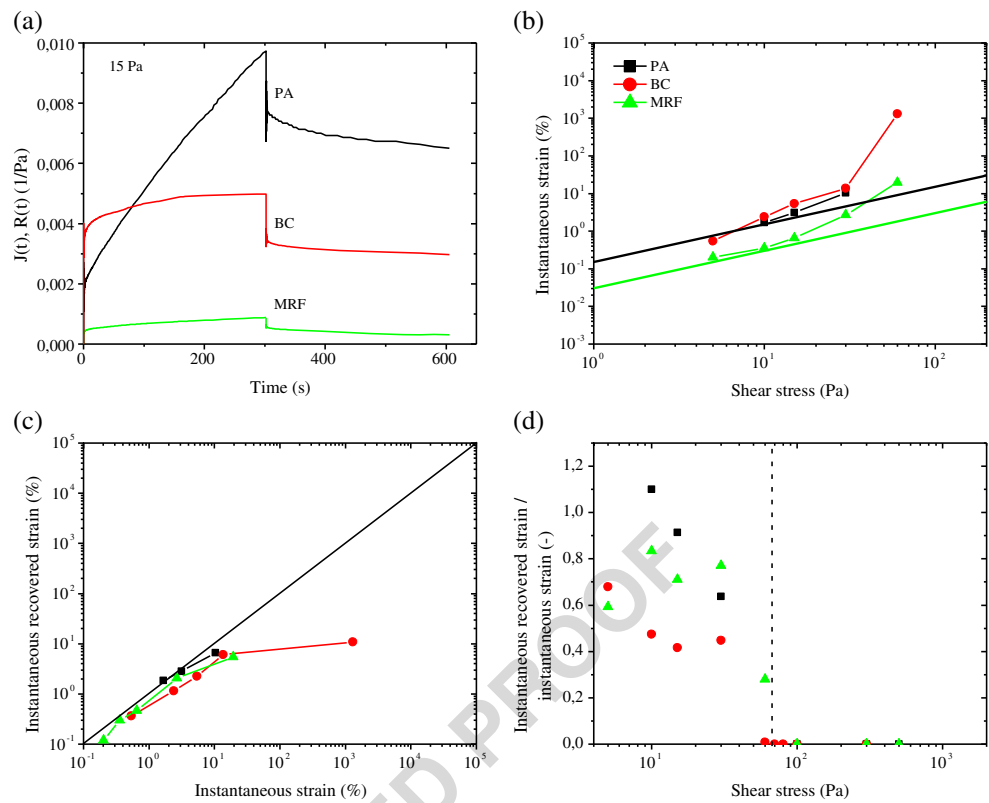
935 Throughout this work, the yielding behavior of conven-
 936 tional MRF has been investigated by using steady shear

Table 2 Same as Table 1 for microgel suspensions (PA), clay suspensions (BC), and MR fluids (MRF) t2.1 Q2

Stress (Pa)	Creep test				Recovery test				t2.2
	J_0 (1/Pa)	η_0 (Pa·s)	J_1 (1/Pa)	t_1 (s)	η_{0r} (Pa·s)	J_{1r} (1/Pa)	t_{1r} (s)	t2.3	
PA									
10	0.0017	120,000	0.00014	7.3	270,000	0.0016	83	t2.4	
15	0.0020	49,000	0.0018	110	44,000	0.0012	24	t2.5	
30	0.0034	23,000	0.00247	32	19,000	0.0024	96	t2.6	
60	0	250	0	–	240	0.0038	200	t2.7	
100	0	35	0	–	32	0	–	t2.8	
300	0	8.1	0	–	8.2	0	–	t2.9	
500	0	2.4	0	–	2.3	0	–	t2.10	
BC									
5	0.0011	200,000,000	0.00057	86	520,000	0.00039	43	t2.11	
10	0.0025	570,000	0.00098	31	520,000	0.0056	590	t2.12	
15	0.0036	400,000	0.00079	21	93,000	0.0011	0.45	t2.13	
30	0.0056	3,900,000	0.0047	30	38,000	0.0015	0.45	t2.14	
60 ^a	–	–	–	–	1,400	0.00045	0.46	t2.15	
70	0	7.5	0	–	7.2	0	–	t2.16	
80	0	0.87	0	–	0.78	0	–	t2.17	
100	0	0.39	0	–	0.34	0	–	t2.18	
300	0	0.11	0	–	0.099	0	–	t2.19	
MRF									
5	0.00046	4,900,000	0.00072	96	610,000	0.00052	67	t2.20	
10	0.00037	560,000,000	0.0018	390	3,900,000	0.00128	230	t2.21	
15	0.00044	1,000,000	0.00015	41	890,000	0.00025	56	t2.22	
30	0.00089	510,000	0.00011	8.9	390,000	0.0005	0.46	t2.23	
60 ^a	–	–	–	–	23,000	0.00056	0.46	t2.24	
100	0	∞	5.7	710	150	0	–	t2.25	
300	0	51	0.75	29	46	0	–	t2.26	
500	0	2.8	0	–	2.8	0	–	t2.27	

MR fluids investigated in this table are different to those reported in Table 1 t2.28

Fig. 12 Characterization of the preyield regime and onset of nonlinearity in PA, BC, and MRF systems: **a** compliance and recoil functions in the preyield regime, **b** instantaneous strain as a function of the applied shear stress. *Solid lines* are taken from the low-strain storage modulus. **c** Instantaneously recovered strain as a function of the instantaneous strain at the onset of creep, **d** ratio between the instantaneously recovered strain and the instantaneous strain as a function of the shear stress



937 and creep–recovery tests, in order to elucidate if these
 938 fluids exhibit time-dependent phenomena like aging and
 939 thixotropy. At very low stress levels, MR fluids behave in
 940 the linear viscoelastic regime and evolve towards nonlin-
 941 ear viscoelastic, viscoplastic, and plastic responses when
 942 the stress value is increased. In steady shear flow, a plas-
 943 tic fluid behavior is found when the imposed stress is larger
 944 than the so-called yield stress. Finally, creep–recovery test
 945 showed that MR fluids might involve the aging phenom-
 946 ena akin to thixotropic fluids at low shear stresses, while
 947 an almost non-thixotropic behavior is exhibited at higher
 948 stresses.

949 **Conclusions**

950 In the literature, tests involving MR fluids typically focus
 951 on the response at shear rates over 1 s^{-1} (See et al. 2004).
 952 However, MR fluids are demonstrated to deviate from plas-
 953 tic fluid models (Bingham, Herschel–Bulkley, etc.) because
 954 the latter assume that the MR fluid operating in the preyield
 955 regime does not deform at all if the applied stress is below
 956 a critical yield stress value (Berli and de Vicente 2012).
 957 In this sense, unsteady creep tests are found to be interest-
 958 ing because they do actually provide further insight into the
 959 yielding mechanism under the presence of magnetic fields.
 960 Indeed, experiments reported here demonstrate that MR

fluids do *creep* even under the presence of stresses below
 the “yield” stress.

In the case of dilute MR fluids subjected at very small
 stress levels, the instantaneously recovered strain is antic-
 ipated to be very similar to the instantaneous strain as
 expected from the linear viscoelasticity theory. This is so
 because field-induced structures slightly deform under the
 applied stress and later recover. In this situation, particle
 aggregates fully connect the plates, generating an elastic
 response that is later released when the stress is removed.
 The stresses investigated in the first part of this work are
 generally too large to observe this region. See et al. (2004)
 reported that the linear response occurs for strains of the
 order of 0.1 % or smaller.

For larger stresses, the energy used to stretch the field-
 induced structures is not completely stored, and partial dis-
 sipation occurs. This finding has been previously described
 in the literature by Otsubo and Edamura (1994) and Li et al.
 (2002) and interpreted by the deformation of clusters of
 particles arranged in a BCT lattice. In general, this is pos-
 sibly due to the existence of structures that are attached at
 only one plate or are completely free (i.e., unattached). The
 deformations of free and unattached chains are expected to
 generate a plastic response.

For stresses very close to the yield stress, the stored
 energy is consumed, and the field-induced structure changes
 to another metastable configuration. The suspension is

988 almost instantaneously strained without viscous flow, and
 989 in this case, the MR fluid will not exhibit an elastic recovery.
 990 The MR fluid behaves as a plastic fluid and exhibits a
 991 stepwise increase in the strain during the creep period.

992 For very large stresses, the field-induced structure is
 993 destroyed, and the system flows with a low viscosity level.
 994 Obviously, the system does not recover the strain upon the
 995 cessation of the stress.

996 Experiments reported here basically concern systematic
 997 creep tests with different stress values at a constant time
 998 of rest (waiting time). With this, it is possible to study the
 999 solid–liquid transition. However, MR fluids and soft glassy
 1000 systems, in general, exhibit two directly related character-
 1001 istics, namely, jamming and aging, that are mechanically
 1002 manifested by the yielding and thixotropic behavior. In our
 1003 opinion, to better understand the aging of these systems,
 1004 future work should involve the study of the effect of the time
 1005 of rest.

1006 **Acknowledgments** This work was supported by MICINN MAT
 1007 2010-15101 project (Spain), by the European Regional Development
 1008 Fund (ERDF), and by Junta de Andalucía P10-RNM-6630 and P11-
 1009 FQM-7074 projects (Spain). CB also acknowledges the financial
 1010 support from the Universidad Nacional del Litoral and the Consejo
 1011 Nacional de Investigaciones Científicas y Técnicas, Argentina.

1012 References

- 1013 Barnes HA (1999) The yield stress—a review or everything flows. *J*
 1014 *Non-Newton Fluid Mech* 81:133–178
- 1015 Barnes HA, Nguyen QD (2001) Rotating vane rheometry—a review. *J*
 1016 *Non-Newton Fluid Mech* 98:1–14
- 1017 Berli CLA, de Vicente J (2012) A structural model for magnetorheology. *Appl Phys Lett* 101:021903
- 1018 Berli CLA, Quemada D (2000) Rheological modeling of microgel
 1019 suspensions involving solid–liquid transition. *Langmuir* 16:7968–
 1020 7974
- 1021 Brady JF (1993) The rheological behavior of concentrated colloidal
 1022 dispersions. *J Chem Phys* 99:567–581
- 1023 Chotpattananont D, Sirivat A, Jamieson AM (2006) Creep and recovery
 1024 behaviors of a polythiophene-based electrorheological fluid.
 1025 *Polymer* 47:3568–3575
- 1026 Christopoulou C, Petekidis G, Erwin B, Cloitre M, Vlassopoulos D
 1027 (2009) Ageing and yield behavior in model soft colloidal glasses.
 1028 *Phil Trans R Soc A* 367:5051–5071
- 1029 Coussot P, Nguyen QD, Huynh HT, Bonn D (2002) Viscosity bifurca-
 1030 tion in thixotropic, yielding fluids. *J Rheol* 46:573–589
- 1031 Coussot P, Tabuteau H, Chateau X, Tocquer L, Ovarlez G (2006)
 1032 Aging and solid or liquid behaviour in pastes. *J Rheol* 50:975–994
- 1033 Craciun L, Carreau PJ, Heuzey M-C, van de Ven TGM, Moan M
 1034 (2003) Rheological properties of concentrated latex suspensions
 1035 of poly(styrene-butadiene). *Rheol Acta* 42:410–420
- 1036 de Vicente J, González-Caballero F, Bossis G, Volkova O (2002) Nor-
 1037 mal force study in concentrated carbonyl iron magnetorheological
 1038 suspensions. *J Rheol* 46(5):1295–1303
- 1039 de Vicente J, Klingenberg DJ, Hidalgo-Álvarez R (2011) Magnetorhe-
 1040 ological fluids: a review. *Soft Matter* 7:3701–3710
- de Vicente J, Stokes JR, Spikes HA (2006) Soft lubrication of model
 hydrocolloids. *Food Hydrocolloids* 20:483–491
- Derec C, Ajdari A, Lequeux F (2001) Rheology and aging: a simple
 approach. *Eur Phys J E* 4:355–361
- Derec C, Ducouret G, Ajdari A, Lequeux F (2003) Aging and nonlin-
 ear rheology in suspensions of polyethylene oxide-protected silica
 particles. *Phys Rev E* 67:061403
- Gutowski IA, Lee D, de Bruyn JR, Frisken BJ (2012) Scaling
 and mesostructure of Carbopol dispersions. *Rheol Acta* 51:441–
 450
- Heyes DM, Sigurgeirsson H (2004) The Newtonian viscosity of con-
 centrated stabilized dispersions: comparisons with the hard sphere
 fluid. *J Rheol* 48:223–248
- Laurati M, Egelhaaf SU, Petekidis G (2011) Nonlinear rheology of
 colloidal gels with intermediate volume fraction. *J Rheol* 55:673–
 706
- Li WH, Du H, Chen G, Yeo SH (2002) Experimental investigation of
 creep and recovery behaviors of magnetorheological fluids. *Mater*
Sci Eng A 333:368–376
- Moller PCF, Fall A, Bonn D (2009b) Origin of apparent viscosity in
 yield stress fluids below yielding. *Eur Phys Lett* 87:38004
- Moller PCF, Fall A, Chikkadi V, Derks D, Bonn D (2009a) An attempt
 to categorize yield stress fluid behaviour. *Phil Trans R Soc A*
 367:5139–5155
- Moller PCF, Mewis J, Bonn D (2006) Yield stress and thixotropy: on
 the difficulty of measuring yield stress in practice. *Soft Matter*
 2:274–283
- Otsubo Y, Edamura K (1994) Creep behavior of electrorheological
 fluids. *J Rheol* 38:1721–1733
- Petekidis G, Vlassopoulos D, Pusey PN (2003) Yielding and flow of
 colloidal glasses. *Faraday Discuss* 123:287–302
- Petekidis G, Vlassopoulos D, Pusey PN (2004) Yielding and flow
 of sheared colloidal glasses. *J Phys Condens Matter* 16:3955–
 3963
- Pham KN, Petekidis G, Vlassopoulos D, Egelhaaf SU, Poon WCK,
 Pusey PN (2008) Yielding behavior of repulsion- and attraction-
 dominated colloidal glasses. *J Rheol* 52(2):649–676
- Quemada D (1977) Rheology of concentrated disperse systems and
 minimum energy dissipation principle I. Viscosity–concentration
 relationship. *Rheol Acta* 16(1):82–94
- Quemada D (1998) Rheological modelling of complex fluids: I. The
 concept of effective volume fraction revisited. *Eur Phys J Appl*
Phys 1:119–127
- Quemada D (2008) Aging, rejuvenation, and thixotropy in complex
 fluids: time-dependence of the viscosity at rest and under constant
 shear rate or shear stress. *Appl Rheol* 18:53298
- See H, Chen R, Keentok M (2004) The creep behaviour of field-
 responsive fluids. *Colloid Polym Sci* 282:423–428
- Segovia-Gutiérrez JP, Berli CLA, de Vicente J (2012) Non-linear vis-
 coelasticity and two-step yielding in magnetorheology: a colloidal
 gel approach to understand the effect of particle concentration. *J*
Rheol 56(6):1429–1448
- Segovia-Gutiérrez JP, de Vicente J, Hidalgo-Álvarez R, Puertas AM
 (2013) Brownian dynamic simulations in magnetorheology. *Soft*
Matter. doi:10.1039/C3SM00137G
- Tadros TF (1987) *Solid/liquid dispersions*. Academic, London, p 293
- Trappe V, Prasad V, Cipelletti L, Segre PN, Weitz DA (2001) Jam-
 ming phase diagram for attractive particles. *Nature* 411:772–
 775
- Volkova O, Cutillas S, Bossis G (1999) Shear banded flows and
 nematic-to-isotropic transition in ER and MR fluids. *Phys Rev Lett*
 82:233–236